Journal of Optoelectronics and Advanced Materials Vol. 1, No. 1, March 1999, p. 27-36

TIN-DOPED ARSENIC SELENIDE GLASSES

M. Iovu, S. Shutov
Institute of Applied Physics, Center of Optoelectronics, 1 Academiei Str.
MD-2028 Chisinau, Moldova

The experimental results of electrical conduction, optical absorption, steady-state and transient characteristics of photoconductivity in bulk and amorphous thermally deposited chalcogenide As_2Se_3:Sn and AsSe:Sn thin films are presented. The tin impurity introduced during thermal synthesis of the starting material As_2Se_3 and AsSe has larger effect on transient rather than on steady-state characteristics of photoconductivity. The charge carrier transport characteristics in these materials are described in the frame of the multiple-trapping model, widely accepted for the amorphous semiconductors. The effect of tin impurity on both extended and localized electronic states are revealed. The tin impurities are also responsible for the photostructural changes of optical properties in AsSe-doped thin films.

(Received January 12, 1999; accepted February 2, 1999)

1. Introduction

The glasses of composition As_2Se_3:Sn and AsSe:Sn are important both for understanding of the relation between the atomic structure, of the optical and electrophysical characteristics and for applications in photonics and optoelectronics. It is well known that impurities have little effect on the electrical characteristics of chalcogenide glassy semiconductors (CGSs), if introduced during thermal synthesis of the glass. At the same time, though the "cold" doping (modification) process, when impurity was added to a substance far from equilibrium, some additives could be made electrically active [1]. In thermally deposited amorphous CGSs films, whose structure exhibits a higher level of disorder than the bulk glass, the incorporation of impurity atoms is more easily accessible. For example, modification of As_2Se_3 with Bi and Sn leaves the Fermi-level practically unaffected [1], whereas in sputtered amorphous films As_2Se_3: Bi_x films (x=0.001; 0.01 and 0.1) significant changes of optical and transport properties have been found [2]. Recently, the effect of copper on electroconductivity, optical bandgap and photosensitivity of bulk glasses and thin films of $Cu_x(AsSe_{1.4}I_{0.2})_{100-x}$ (x=0.1, 5, 10, 15 at. %) alloys was investigated [3]. Similarly, in thermally deposited As_2Se_3:Sn_x (x=0.1 . . . 3.5 at. %) and AsSe:Sn_y (y=1 . . . 10 at. %) thin films photosensitivity was shown to be much higher than that of bulk glass [4].

The use of As_2Se_3:Sn layers in film structures for electrophotographic recording of optical information [5] and holography [4] increases substantially the photosensitivity. Tin impurity in amorphous AsSe thin films stabilizes the parameters of the recording media due to more rigid network of the doped glasses and thus opens the way for important applications in optoelectronics [6]. Recently, M. Popescu et al. [7] has shown that UV excimer laser irradiation of tin-doped AsSe thin films allow to get a reversibility of the photo-amorphization phenomena, as a function of the UV beam energy, which is also very important for recording of optical information.

Measurements of the time-of-flight in As_2Se_3:Sn films have recently established [8] that adding tin to As_2Se_3 substantially increases the drift mobility and slows down recombination. The obtained results indicate the variation in occupation of deep localized centres and also explain the known effect of photosensitivity enhancement when ternary chalcogenide glassy alloys are used in multilayer structures for optical information storage.

This paper deals with the investigations of influence of tin doping on electrical, optical, steady-state and transient characteristics of photoconductivity in As_2Se_3 and AsSe bulk and amorphous thin films. The experimental techniques included measurements of optical reflection (fundamental absorption region, 2.2 to 6.2 eV, optical transmission, stationary and non-stationary electrical, photoconductivity and photocapacitance (the region of edge and sub-band absorption)

characteristics. Some results of photodarkening process under the He-Ne laser illumination of AsSe thin amorphous films are presented, too.

2. Experimental

Tin was introduced in an amount of x=0.1-3.5 at.% into the As_2Se_3 and of x=1-10 at.% into the AsSe during thermal synthesis of the initial material for sputtering. Synthesis was conducted by melting the charge in an evacuated quartz cell followed by holding at a temperature of 1100 °C and slow cooling with the furnace switched off. $As_2Se_3:Sn_x$ and $AsSe:Sn_x$ films of thickness 1.0-10.0 μm were obtained by discrete thermal sputtering in vacuum on glass substrates held at 100 °C. For electrical measurements the samples had a sandwich configuration with two sputtered electrodes (gold or aluminium), of which the top electrode was half-transmitting. For optical and photoelectric measurements the spectrometers SPM-2 and MDR-2 with photorecording modules were used. The photoconductivity was also excited by a LGN-108 helium-neon laser, a photoshutter with a 10^{-3} s triggering time was used to switch the light on/off. The intensity of the light ($F_0 = 10^{15}$ $cm^{-2} \cdot s^{-1}$) could be decreased with calibrated filters. Bias illumination ($F=3\times10^{14}$ $cm^{-2} \cdot s^{-1}$) was produced by light from a KGM-100 incandescent lamp. To obtain uniform optical excitation in the sample, the light was passed through an arsenic selenide film filter. The photoconductivity relaxation curves were recorded with a time constant not exceeding 0.3 s on a ENDIM 622 02 X-Y plotter using an U5-11 electrometric amplifier. The photocapacitance was measured by a quasistatic technique at a frequency 10^{-2} Hz. In time-of-flight experiments the photocurrent was excited by a pulse of strongly absorbed light generated by a nitrogen laser (λ=0.34 μm).

3. Experimental results and discussion

3.1. Optical Absorption

The reflectivity spectra of the AsSe (Fig.1, curve 1) and $AsSe:Sn_1$ (curve 2) films in the photon energy range 2 to 6.2 eV show a wide double peak as well as some weaker peculiarities signed by arrows. The spectra are in agreement with the picture known from the literature for the glass of stoichiometric composition As_2Se_3 [9,10].

According to band structure calculations in tight-binding approximation [11] the states near the valence band edge of As_2Se_3 are predominantly on the chalcogen lone-pair ***p*** orbital (low-energy side of the reflectivity peak in Fig. 1), while the high-energy side of the peak is due to $p\sigma$ orbital of the chalcogen atom. Both sides of the reflectivity peak contain the contributions of ***p*** and ***s*** orbitals of arsenic. It is seen from Fig.1 that addition of tin creates considerable changes in the fundamental reflection spectrum lowering the low-energy side of the peak and raising its high-energy side. These modifications indicate that the contributions of the lone-pair and bonding orbitals are changed in favour of the latter. At the same time, taking into account the low tin content (1 at. %) the impurity effect is expected more in the domain of intermolecular interaction [12], when delocalization of lone-pair electrons lowers the energy of valence states, leading to stabilization of the whole system. The valence band edge is shifted by about 0.1 eV as it is clearly seen from Fig. 1.

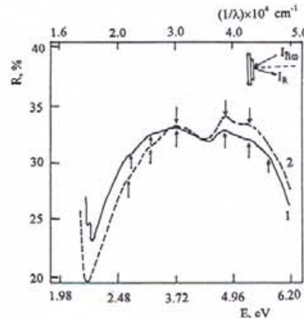

Fig. 1 Reflectivity spectra of AsSe (1) and $AsSe:Sn_1$ (2) thin films.

The spectra of edge optical absorption (Fig. 2a) as well as corresponding photoconductivity spectra (Fig. 2b) of the AsSe films with various content of tin impurity are characteristic of amorphous semiconductors. In the high absorption region close to the beginning of band-to-band optical transitions the absorption coefficient obeys a square-law energy dependence $\alpha \sim (h\nu - E_g^{opt})^2/h\nu$. This dependence, widely known as Tauc plot, gives correct value of the optical gap E_g^{opt} determined as the energy difference between the onsets of exponential tails of the allowed conduction bands [13]. The variation of the E_g^{opt} determined from this relation for various tin content is listed in Table 1 and is shown in the insert of Fig. 2a. Alternatively, the optical gap E_g^{α} may be evaluated as an energy for a given value of absorption coefficient $\alpha=10^3$ cm^{-1} (see Table 1).

It is seen that tin impurity lowers the optical gap, first (to 1 at. %) steeper and then nearly proportional to the tin concentration. This fact indicates that at sufficiently high tin content there are formed new structural units with lower optical threshold energy, the presence of which lowers the mean value of the gap, as in alloys. As the structure of AsSe glass is usually treated on the base of a statistical model build from four local structures $AsSe_3$, $AsSe_2As$, $AsSeAs_2$ and $AsAs_3$ [14], the assumption of formation of structural units with Sn is not inconsistent with the model. From Mössbauer spectroscopic study [15] it was concluded that tin impurity in CG of the As-Se type interacted only with Se atoms and entered the glass matrix with the maximal valence +4 and co-ordination number 6 (as in $SnSe_2$).

Table 1 Energy band parameters, determined for AsSe:Sn_x amorphous films from optical and photoelectrical spectra.

Band parameter	Content of tin in AsSe:Sn_x, at. %					
	0	1	2	3	7.5	10
E_g^{opt}, eV	1.805	1.725	1.716	1.708	1.671	1.625
E_g^{α}, at 10^3 cm^{-1}, eV	1.842	1.765	1.718	1.693	1.625	1.425
Urbach slope, E_0, meV	56.3	50.7	84.0	84.0	51.5	157.0
$E_{ph}(\lambda_{1/2})$, eV	1.86	1.71	1.75	1.73	1.68	1.56

The variation of the optical gap with the tin content was explained in the frame of the structurochemical model, taking into account the most favourable structural units discussed by Myuller [16] as possible constituents of the chalcogenide glasses. The following units, in proportion corresponding to the right composition were used in the model: $AsSe_{1.5}$, As_2Se_2, As_2 and SnSe.

X-ray diffraction measurements were carried out on thin amorphous films by the diffractometric method. The internal distance corresponding to the position of the first sharp diffraction peak (FSDP) shows an increase with the tin content. This distance calculated from the structurochemical model reproduces fairly well the diffraction results. The detailed structurochemical model will be given elsewhere [17].

At intermediate values of the absorption coefficient in the range $h\nu < E_g$ the absorption edge behaves exponentially $\alpha(h\nu) \sim \exp[(h\nu - E_g^{opt})/E_{oo}]$ (Fig.2a). This dependency often called as Urbach edge is characteristic of amorphous semiconductors. The Urbach edge arises from superposition of electron transitions from the valence band tail to extended states of the conduction band (and vice versa). As a rule the more broad valence band tail is dominant, that is, the width E_{oo} is characteristic of it. Between the apparent gap Eg and the tail width E_{oo} a simple correlation exists [18]:

$$Eg = Eg^o - cE_{oo} \tag{1}$$

where Eg^o is the limiting value of the gap for a vanishing small tail width and c is constant (c=5 to 10 for *a*-Si:H) [18]. If the tail width varies with the impurity content (or temperature), the extrapolations of the Urbach edges to higher energies for various impurity concentrations have to cross at a focus, the position of which corresponds to Eg^o. It is seen from Fig. 2 that the slope of the exponential portions decreases with the increase of the tin content, and the largest slope corresponds to undoped AsSe. The correlation (1) fits to all alloys with the values Eg^o=2.15 eV and c=5.2, and the absorption

at the end of the exponential tail is more than 100 times increased. The above described behaviour indicates that tin impurity induces broadening of the band tail states from 0.06 eV for undoped AsSe to 0.16 eV for AsSe:Sn_{10} (see Table 1). This broadening may be caused by formation of new Sn-based structural units as well, which add a compositional disorder to the existing structural one.

The behaviour of the Urbach edge corresponding to Eq. (1) is usually ascribed to the variation of the degree of structural disorder, in fact the medium range ordering, which include both the thermal and frozen-in disorder. Hosokawa et al. [19] observed a fan-like decreasing of the Urbach slope of As_2S_3 and As_2Se_3 in a wide-range temperature interval 25 to 900 °C. Tichá et al. [20] obtained similar behaviour of spectra of glassy As_2S_3 samples under thermal treatment with various quenching rates. The reasons for this behaviour and the role of disorder in formation of the Urbach edge, first stressed by Olley [21], are still under discussion [22]. Here we wish to notice, that the behaviour of the Eq. (1) type if for the first time observed for the case of a chalcogenide glass with varying impurity concentration.

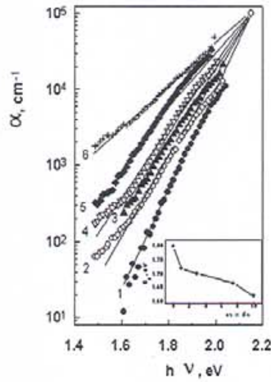

Fig. 2a Edge absorption of AsSe:Sn_x films.
x: 1-0; 2-1.0; 3-2.0; 4-5.0; 5-7.5; 6-10.
Insert: Optical gap vs. tin content.

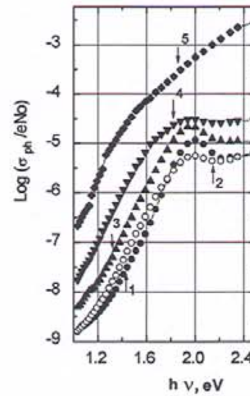

Fig. 2b The photoconductivity spectra for the $As_{50}Se_{50}$:Sn_x thin films.
x: 1-0; 2-2.0; 3-3.0; 4-7.5; 5-10.0.

Photocapacitance spectroscopy technique on the barrier junctions in the AsSe:Sn_x was used to measure optical absorption in the depth of the gap [23]. Nonequilibrium population of holes in deep traps in the space-charge region of the barrier build by a preliminary filling pulse is emitted by exciting light leading to barrier capacitance relaxation. The initial relaxation rate normalized per exciting photon is equivalent to optical absorption coefficient associated with photoemission process. The absorption spectra obtained from photocapacitance measurements in the range $h\nu<1.6$ eV may be associated to defects and impurities and the values of the absorption coefficients may be found by extraction of the exponential part from the apparent absorption values. Evaluation of the excess centre density yields the value (2 to 5)$\times10^{16}$ cm^{-3} [24]. Though the occurrence of the excess absorption peak at 1.53 eV is obviously associated with the addition of tin, the obtained concentrations of optically active centres remain practically at the level of defect density known from ESR measurements (about 10^{17} cm^{-3}).

3.2. Steady-State Conductivity and Photoconductivity

In Fig. 3a the data for dark electrical conductivity, its activation energy and photoelectrical bandgap for bulk samples in the system As_2Se_3:Sn_x are presented. Tin leads to slow increasing of the activation energy E_a from 0.85 eV for As_2Se_3 to 0.96 eV for $As_2Se_3Sn_{3.5}$, with a plateau at about 2 at. % Sn seen in the concentration dependence of E_a. The energy position of the photoconductivity maximum (curve 1 in Fig.3a) slightly changes versus tin content in the alloys. The change of the power index γ of the lux-ampere characteristics ($i_{ph} \sim G^{\gamma}$) with tin concentration at room temperature increases from 25 meV for As_2Se_3 to about 88 meV for x=3.5 at.% Sn with a kink around x=2 at.% Sn. According to X-ray diffraction studies [25] the dopant atom (Sn) inserted into the glass

network increases the thickness of the layered configuration leading to the transition to three-dimensionally ordered network. In the $As_2Se_3:Sn_x$ this transition occurs at about x=2 at. % Sn and is followed by above-mentioned peculiarities in electronic properties.

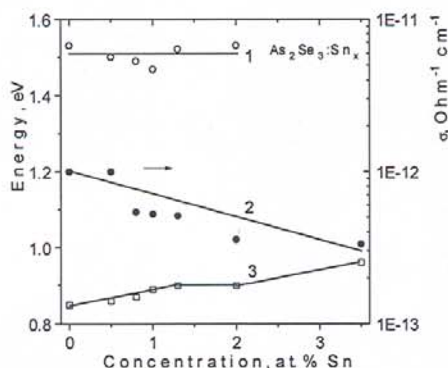

Fig.3a The dependence of photoelectrical band energy E_{ph} *(1), conductivity* σ *(2) and activation energy* E_a *(3) on tin concentration, x, in the system* $As_2Se_3:Sn_x$.

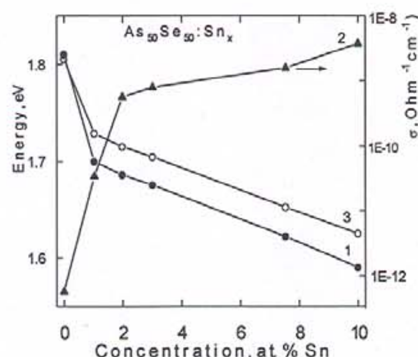

Fig.3b The dependence of photoelectrical band energy E_{ph} *(1), conductivity* σ *(2) and optical band gap* E_g^{opt} *(3) on tin concentration,x, in the system* $AsSe:Sn_x$.

It is seen from the steady-state conductivity results that adding of Sn to As_2Se_3 really has week effect on its electrical properties: the conductivity decreases about three times at the highest Sn concentration and the Fermi level (i.e. the activation energy) slightly shifts up by about 0.1 eV. That is, it appears that Sn is not electrically active impurity.

In Fig.3b the data for electrical conductivity, optical and photoelectrical bandgap for $AsSe:Sn_x$ films are presented. Tin impurity increases the electrical conductivity and lowers the optical bandgap. The spectra of edge optical absorption as well as corresponding photoconductivity spectra of AsSe films with various content of tin impurity are characteristic of amorphous semiconductors. The photoconductivity spectra of $AsSe:Sn_x$ films show an exponential dependence of the long wavelength edge on the photon energy [24]. In contrast to the absorption spectra incorporation of tin is followed by the shift of the photoconductivity spectra to lower energy ahead of the decreasing optical gap E_g^{opt} The shift of E_g^{opt} is about 0.2 eV, while the shift of the photoconductivity edge is 0.6 eV for 10 at. % Sn.

The exponential portion of the photoconductivity spectra extends much deeper into the gap than that of the absorption edge. The photocurrent after adding of tin impurity increases (more than 250 times for 10 at. % Sn). The above peculiarities indicate that the photoconductivity is determined not only by the band tail absorption but also by absorption at deep defect states in the weak absorption region.

3.3. Transient photoconductivity

Chalcogenide glassy semiconductors are known as photosensitive materials for large-area information storage devices. Photoelectrical properties of chalcogenide glasses are usually considered on the basis of charged-defect model [26], in which recombination is described as a tunnelling process between the metastable defect states. Besides, prolonged non-stationary processes due to multiple trapping in quasi continuously distributed in energy gap states are typical for amorphous semiconductors, leading to specific phenomena such as dispersive transport and photoinduced optical absorption.

Dynamics of photocarrier generation and recombination under the condition of non-equilibrium energy distribution of localized carriers is described by [27]:

$$dp(t)/dt=G(t)-(1/\tau_R)p_c(t) - Rp_c(t)p(t), \quad (2)$$

where t is the time, p the total charge density, p_c the density of delocalized carriers, $G(t)$ the generation rate, τ_R the lifetime of delocalized carriers with respect to the monomolecular recombination (MR), R the constant of the bimolecular recombination (BR). The Eq. (2) should be supplemented with the relation between the total charge carrier density $p(t)$ and the density $p_c(t)$ of carriers in delocalizated states. For the case of non-equilibrium (dispersive) regime specific for amorphous semiconductors this relation takes the form [28]:

$$p_c(t) = d/dt\,[\tau(t)\,p(t)], \tag{3}$$

were $\tau(t)$ is the lifetime of free carriers before capture into the "deep" fraction of gap states, the escape from which is improbable until the time t:

$$[1/\tau(t)]=(1/\tau_0)\int_{E^*(t)}^{\infty}[n(E)/N_t]dE. \tag{4}$$

Here τ_0 is the lifetime of free holes before capture into gap states, N_t the total density of localized states, $n(E)dE$ the localized state density in the energy interval from E to $E+dE$ and $E^*(t)$ the demarcation energy below which the region of deep states is located:

$$E^*(t) = kT\,ln[(N_c/N_t)(t/\tau_0)], \tag{5}$$

where N_c is the density of extended states and T the temperature. As usual, holes are considered as mobile carriers, while electrons are assumed to be captured after generation and immobile during the recombination process. A broad dispersion of recombination lifetimes due to multiple trapping of excess carriers in energy-distributed gap states is main peculiarity of Eq. (2). The solution of Eq. (2) for an important case of exponential trap distribution $n(E)=(N_t/E_0)exp(-E/E_0)$, with the dispersion parameter $\alpha=kT/E_0$, yields formulae for increasing and decreasing of the free carrier density $p_c(t)$ after the light is switched on/off, which are summarized in Table 2. As the transient photocurrent $i_{ph}\sim p_c(t)$, several time domains can be revealed in the transient curves, each of which corresponds to a power dependence of photocurrent upon time and is determined by capture or recombination of excess carriers in MR or BR regime. The transition to MR regime at the moment $t=t_1$ is determined by the expression:

$$t_1 = \tau_0\,(Nt/Nc)\,(\tau_R/\tau_0) \tag{6}$$

Table 2 Expressions for the density of delocalized carriers, $p_c(t)$.

	Capture	MR regime	BR regime
Rise	$G_0\tau_0(\frac{N_c}{N_t})^{\alpha}(\frac{t}{\tau_0})^{\alpha}$	—	$(\frac{G_0}{R})^{1/2}(\frac{N_c}{N_t})^{\alpha/2}(\frac{t}{\tau_0})^{-(1-\alpha)/2}$
Steady-state	—	$G_0\tau_R$	$N_c(\frac{G_0}{RN_cN_t})^{1/(1+\alpha)}$
Decay	$p_0\alpha(\frac{N_c}{N_t})^{\alpha}(\frac{t}{\tau_0})^{-(1-\alpha)}$	$p_0\alpha(\frac{N_t}{N_c})^{\alpha}(\frac{\tau_R}{\tau_0})^{2}(\frac{t}{\tau_0})^{-(1+\alpha)}$	$\frac{\alpha}{Rt}$

Photoconductivity kinetics was studied in AsSe, As_2Se_3, AsSe:Sn and As_2Se_3:Sn films deposited onto glass substrates by thermal flash-evaporation. The photocurrent was generated in a step-function mode by He-Ne laser light and was registered by an oscilloscope and a chart-recorder. A typical picture of the photocurrent transients is shown in Fig. 4 for various intensities (a) and temperatures (b). In Fig. 5 the rise and decay curves of Fig. 4a are replotted in double-logarithmic scale to visualize the power-law portions of the transients discussed below.

Over the initial part up to the moment t_1 the photocurrent rise is governed by the capture process, while recombination so far is not significant: $i_{ph}\sim G\cdot t^{\alpha}$ (Fig. 5a). Further behaviour of the transients depends on excitation intensity. At low intensities (corresponding to MR) the photocurrent monotonously increases and reaches the steady-state value. At higher exposure intensities a

quasi-stationary part is observed, which at certain moment is followed by a decreasing portion of the transient, where the BR mechanism is dominant. Along this portion $i_{ph}\sim G^{1/2}\cdot t^{[(1-\alpha)/2]}$. At highest excitation level the relaxation is governed by BR and the quasi-stationary portion of photocurrent is absent ("an overshoot", see Fig. 4a).

The photocurrent decay depends on the initial density of photogenerated charge carriers. If during the generation pulse the total filling of gap states is not achieved then an initial portion of the decay governed by capture process exist and the recombination is delayed. Over this portion $i_{ph}\sim i_{ph0}\cdot t^{(1-\alpha)}$ where i_{ph0} is the photocurrent at the moment when the light is switched off (Fig. 5b). At low generation intensities (MR regime) the starting portion turns into final decay, along which $i_{ph}\sim i_{ph0}\cdot t^{e-(1+\alpha)}$. If the generation intensity provides the BR regime, then an intermediate portion exists, where $i_{ph}\sim i_{ph0}\cdot t^{-1}$. The above described behaviour of photocurrent kinetics is in good agreement with the experimental curves of transient photocurrents for a set of generation rates presented in Fig. 5. From these the dispersion parameter α=0.67 can be estimated for AsSe, which determines the energy parameter of the density-of-states distribution E_0=0.037 eV.

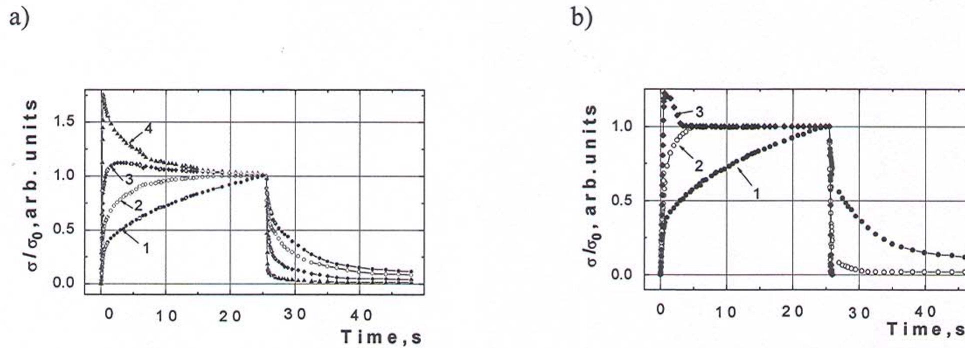

Fig. 4 Photoconductivity relaxation in the $As_{50}Se_{50}$ films at various intensities F (a) and Temperatures T (b). Light is switched on at t=0 and off at t=26 s. (a) F, $cm^{-2}\cdot s^{-1}$: 1 - $5.3\cdot10^{11}$, 2 - $2.4\cdot10^{12}$, 3 - $1.5\cdot10^{13}$, 4 - $6.5\cdot10^{14}$. (b) T, K: 1 – 289, 2 - 341, 3 - 393.

The straight lines calculated with α=0.67 as asymptotics of the power-law parts in the rise and the decay of photocurrent are plotted in Fig. 5. For As_2Se_3 and As_2Se_3:Sn the values of α are 0.54 and 0.70, respectively. The fact that the complex picture of the photocurrent kinetics can be described by single parameter justifies the use of the model of multiple-trapping controlled recombination. The variation of the kinetics with temperature (Fig. 4b) corresponds to the predictions of the model as well, as the transition moment t_1 is exponentially shifted to shorter times as the temperature is increased. It is worth noting the important role, which capture plays in photoconductivity of amorphous semiconductors, determining the specific initial portions of relaxation. Capture enhancement leads to the delay of recombination and to shift of the moment t_1 to longer times.
The shortest time t_1, corresponding to the onset of recombination in investigated glasses, appears for the stoihiometry composition As_2Se_3 ($t_1=10^{-2}$ s), it is about 3.3 s in AsSe films (containing excess As atoms) and becomes longer (up to 10...15 s) in As_2Se_3 films doped with 1 at.% Sn. The time delay of recombination with introduction of 1.0 at. % Sn in As_2Se_3 was also observed in time-of-flight experiments [8]. Close values were obtained for the times corresponding to the onset of intense recombination (2.3 and 11.8 for As_2Se_3 and $As_2Se_3:Sn_1$, respectively). Additional evidence in support of a delay of recombination in $As_2Se_3:Sn_1$ samples comes from the effect of constant bias illumination [8]. Bias illumination increases the decay rate, which is growing with increasing illumination intensity, by accelerating photoionization and recombination of localized nonequilibrium current carriers (Table 3).

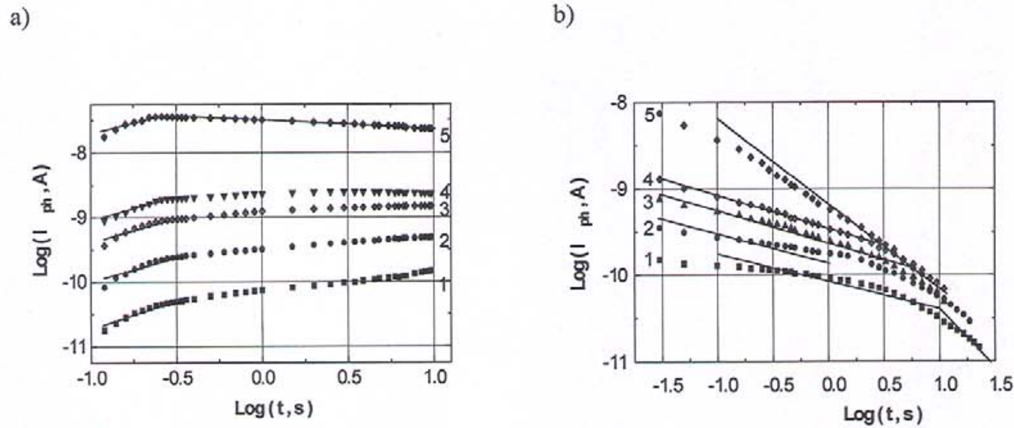

Fig.5 Double-logarithmic plot of photocurrent rise (a) and decay (b) in the $As_{50}Se_{50}$ film at various light intensities F, $cm^{-2}\cdot s^{-1}$: 1 - $5.3\cdot 10^{11}$, 2 - $2.4\cdot 10^{12}$, 3 - $6.6\cdot 10^{12}$, 4 - $1.5\cdot 10^{13}$, 5 - $6.5\cdot 10^{14}$. Straight line portions are calculated with $\alpha = 0.67$ (see text for details).

The increase of the role of capture in the characteristics of the drift mobility under nonstationary conditions of dispersion transport has been noted previously for arsenic sulphide films doped with tin up to 3.0 at.% [29]. The observed effect of transient processes strongly affected by impurity atoms is in contrast to well-known insensitivity of equilibrium characteristics of glassy semiconductors to doping. Enhancement of capture in a given time domain strongly affects the dependence of the transients on light intensity and temperature as well as on optical bias. For example, the 'overshoot' in the rising part of the photocurrent (Fig. 4a) disappears in Sn-doped samples.

Table 3 The experimental values of the recombination time t_R for As_2Se_3 and $As_2Se_3:Sn_{1.0}$ thin films.

Specimen	E x 10^4, V/cm	t_R, s (without optical bias)	t_R, s (with optical bias)
As_2Se_3	4	6.0	1.7
As_2Se_3	8	2.3	-
$As_2Se_3:Sn_{1.0}$	8	11.8	1.8
$As_2Se_3:Sn_{1.0}$	13	10.0	1.4
$As_2Se_3:Sn_{1.0}$	19	5.7	0.9

3.4. Photo-Induced Changes in Optical Properties

Amorphous chalcogenides As-Se thin films exhibit a wide variety of physical and chemical changes during the illumination by an band-gap photon energy $h\gamma \geq E_g$. The photo-induced changes in optical properties induce the shift of the optical absorption edge to lower energies and decreasing of the transmittance at fixed wavelength after irradiation and makes the chalcogenide thin films very important for recording of optical information. The origin of reversible and irreversible photostructural changes in chalcogenide glasses was explained by M. Popescu et al. [30], H. Fritzsche [31], A. Kolobov and G. Adriaenssens [32]. Such photo-induced changes are caused by the processes of reversible local ordering-disordering of glass structure, including the amorphization phenomena [7], or irreversible ordering up to crystallization. In some cases the electronic processes responsible for the photostructural changes are taken into account [32].

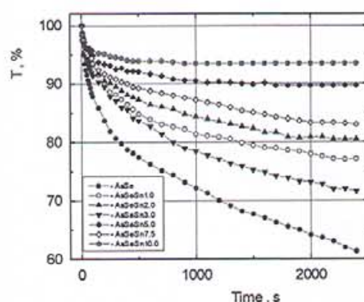

Fig. 6a The transmittance of AsSe:Sn thin films vs. time during laser illumination.

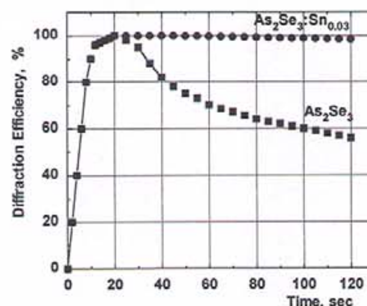

Fig. 6b The kinetics of diffraction efficiency rise for the As_2Se_3 and As_2Se_3:$Sn_{0.03}$ thin films.

As we have mentioned, tin impurity in amorphous AsSe thin films lead to some stabilizing effects of the parameters of the recording media due to more rigid network of the doped glasses [4, 25]. In our case we measured the changes of transmitance of AsSe:Sn thin films during He-Ne laser (λ=0.63 μm) illumination as well as before and after light exposure. The holographic studies were performed by means of lensless Fourier hologram recording.

During the laser illumination of AsSe:Sn thin films the transmittance becomes lower and the fundamental absorption edge shifts to lower energies, i.e. the effect of photodarkening takes place. The effect of photodarkening is more pronounced in AsSe thin films without tin content. The increase of optical absorption of AsSe:Sn thin films exposed to prolonged laser-light illumination is shown in Fig. 6a.

Light-induced photodarkening of the films exhibits fast ***($\Delta T\approx 20$ %, t =300 s)*** and slow (another ***$\Delta T\approx 20$ %, t = 2400 s)*** stages of the process. Doping by tin gradually removes the slow stage of the photodarkening producing a stabilizing effect on the structure of the ***AsSe*** film. A progress in the stability of the diffraction efficiency for the AsSe thin films doped with tin was observed (Fig. 6b). That behaviour may be connected with the peculiarities of the structure of the AsSe and AsSe:Sn thin films, especially with the appearance of the new structural molecular units as a result of tin doping. The more detailed these results will be discussed in the later publication [17].

4. Conclusions

The spectra of optical absorption of amorphous AsSe films doped with 1 to 10 at. % Sn are studied in a wide interval of excitation energy involving electron transitions associated both with deep states of the valence band and deep localized states in the mobility gap. It is shown that tin, an impurity with valence and co-ordination different from those of the atoms of the host glass, influences absorption more or less in all regions of the investigated spectrum. The changes in the reflectivity spectrum associated with optical transitions from the deep states of the valence band suggest the modification of intermolecular interaction in the glass matrix. In the absorption region interesting results are obtained indicating for the first time the validity of the correlation between the widths of the gap and that of the band tail for the case of doping of As-Se chalcogenide glasses.

It was shown also, that tin impurity introduced into As-Se chalcogenide glasses during thermal synthesis has a much stronger effect on the non-stationary characteristics of the photoconductivity than on the equilibrium parameters. The influence is based on the increased role of capture in deep localized states as a result of the introduction of tin. Intensification of capture, which determines the slow initial relaxation stages which are specific for the chalcogenide glasses, results in a delay of recombination onset in doped samples and increases the lifetime of the photoexcited state after the light is removed. The optical bias influences the occupation of deep localized states giving the increase of drift mobility and decrease of the recombination time.

The photodarkening process in the AsSe:Sn thin films may be used for recording of optical and holographic information. Tin impurity in amorphous AsSe thin films stabilizes the parameters of

the recording media due to more rigid network of the doped glasses and that opens the way for important applications in optoelectronics.

Acknowledgments

The authors thank to Dr. M. Popescu (INFM-Bucharest) for discussions, which highlighted and stimulated this work.

References

[1] Kolomiets B.T., Averyanov V.L., in Physics of Disordered Materials (New-York, London) p.663(1985).
[2] Kalmikova N.P., Mazets T.F., Smorgonskaya E.L., Tsendin K.D., Fizica i Tehnika Poluprov. (russ.) **28**, 297(1989).
[3] Lukič S.R., Petrovič D.M., Petrovič A.F., J. Non-Cryst. Solids **241**, 74(1998).
[4] Buzdugan A.I., Iovu M.S., Popescu A.A., Cherbari P.G., Balkan Phys. Letters **1**, 7(1994).
[5] Korshak O.Ya., Panasyuk L.M., Rotar V.K., Fulga V.I., in Electrography-88, Moscow, **2**, 51(1988).
[6] Iovu M.S., Popescu M., Syrbu N.N. et al., Abstr. of the 5-th Symp. of Optoelectronics, Bucharest, Sept. 23-25, 20(1998).
[7] Popescu M., Sava F., Lőrinczi L., Andriesh A., Iovu M., Rebeja S., Shutov S.,Vateva E., Skordeva E., Bradaczek H., Koch P.-J., Obst S., Proceedings Intern. Conf. ROCAM'97, Analele Universitatii Bucuresti, **XLVI**, 199(1997).
[8] Iovu M.S., Shutov S.D., Tóth L., phys. status solidi B **195**, 145(1996).
[9] Andriesh A.M., Sobolev V.V., Lerman I.N., Izv. Akad. Nauk MSSR, ser. fiz.mat. (russ.) **6**, 91(1967).
[10] Drews R.E., Emerald R.L., Slade M.L., Zallen R. Solid State Communic. **10**, 293(1972).
[11] Bullet D.W., Phys.Rev. B **14**, 1683(1976).
[12] Watanabe Y., Kawazoe H., Yamane M. J. Non-Cryst. Solids **95-96**, 365(1978).
[13] Jakson W.B., Kelso S.M., Tsai C.C., Allen J.W., Oh S.-J., Phys. Rev. B**31**, 5187(1985).
[14] Connell G.A.N., Lucovsky G., J. Non-Cryst.Solids **31**, 123(1978).
[15] Seregin P.P., Sivcov V.L., Vasiliev A.N., Fizika i Tehnica Poluprov. (russ.) **8**, 2270(1974).
[16] Myuller R.L., Solid State Chemistry, Ed. by Z.U. Borisova (Consultants Bureau, New York) p. 1(1966)
[17] Popescu M. et al. (to be published).
[18] Cody G.D., Tiedje T., Abeles B., Brooks B., Goldstein Y., Phys. Rev. Lett. **47**, 1480(1981).
[19] Hosokawa S., Sakaguchi Y., Hiasa H., Tamura K., J.Phys.: Condens. Matter. **3**, 6673(1991).
[20] Tichá H., Tichý L., Klikorka J., Špaèek V., Solid State Commun. **68**, 575(1988).
[21] Olley J.A., Solid State Commun. **13**, 1437(1973).
[22] O'Leary K., Zukotinsky S., Perz J.M., Phys. Rev. B **51**, 4143(1995).
[23] Vasiliev I.A., Shutov S.D., Sov. Semiconductors, **32**, 439(1998).
[24] Iovu M.S., Popescu M., Syrbu N.N., Shutov S.D., Vasiliev I.A., Rebeja S., Colomeico E., Proceedings CAS'98, Sinaia, **1**, p.105 (1998).
[25] Andriesh A., Popescu M., Iovu M. et al., Proceedings CAS'95, Sinaia, p.83 (1995).
[26] Mott N.F., Davis E.A., Electron Processes in Non-crystalline Materials, Clarendon Press, Oxford (1979).
[27] Arkhipov V.I., Iovu M.S., Rudenko A.I., Shutov S.D., Sov. Phys. Semicond. **19**, 6(1985).
[28] Arkhipov V.I., Rudenko A.I., Phil.Mag. B **45**, 189 (1982).
[29] Andriesh A.M., Gerasimenko V.S., Ivaschenko Yu.N., Iovu M.A., Iovu M.S., Mironos A.V., Smirnov V.L., Chernii M.R., Shutov S.D., J. de Physique **42**, Coll.C4, 963(1981).
[30] Popescu M., Andriesh A., Chumash V., Iovu M., Tsiuleanu D., Shutov S., Physics of Chalcogenide Glasses (roum.), Chisinau-Bucuresti, Stiintsa (1996).
[31] Fritzsche H., Phil. Mag. B **68**, 561(1993).
[32] Kolobov A.V., Adriaenssens G.A., Phil. Mag. B **69**, 21(1994).